

Article

Not peer-reviewed version

Multiple Diffraction in a Basic Co-Rich Decagonal Al-Co-Ni Quasicrystal

[Changzeng Fan](#)*

Posted Date: 2 December 2025

doi: 10.20944/preprints202512.0094.v1

Keywords: multiple diffraction; decagonal quasicrystal; single crystal X-ray diffraction; synchrotron radiation; kinematical theory



Preprints.org is a free multidisciplinary platform providing preprint service that is dedicated to making early versions of research outputs permanently available and citable. Preprints posted at Preprints.org appear in Web of Science, Crossref, Google Scholar, Scilit, Europe PMC.

Copyright: This open access article is published under a [Creative Commons CC BY 4.0 license](#), which permit the free download, distribution, and reuse, provided that the author and preprint are cited in any reuse.

Disclaimer/Publisher's Note: The statements, opinions, and data contained in all publications are solely those of the individual author(s) and contributor(s) and not of MDPI and/or the editor(s). MDPI and/or the editor(s) disclaim responsibility for any injury to people or property resulting from any ideas, methods, instructions, or products referred to in the content.

Article

Multiple Diffraction in a Basic Co-Rich Decagonal Al-Co-Ni Quasicrystal

Changzeng Fan ^{1,2}

¹ State Key Laboratory of Metastable Materials Science and Technology, Yanshan University, Qinhuangdao 066004, China; chzfan@ysu.edu.cn

² Hebei Key Laboratory for Optimizing Metal Product Technology and Performance, Yanshan University, Qinhuangdao 066004, China

Abstract

To reveal its influence on quasicrystal structure analysis, multiple diffraction (MD) effects in a basic Co-rich decagonal Al-Co-Ni quasicrystal have been investigated in-house and with synchrotron radiation. Two weak reflections were chosen as the main reflections (**P**) in the in-house measurements and 40° ψ -scans of one main reflection have been performed with synchrotron radiation. As well known for periodic crystals and the *i*-quasicrystal, it is also observed for this *d*-quasicrystal that the intensity of the main reflection may significantly increase if the simultaneous (**H**) and the coupling (**P-H**) reflections are both strong. The occurrence of MD events during collection of a full data set as well as the ψ -scans measurements have been studied based on an average structure model and the kinematical MD theory.

Keywords: multiple diffraction; decagonal quasicrystal; single crystal X-ray diffraction; synchrotron radiation; kinematical theory

1. Introduction

Multiple diffraction happens when two or more diffraction beams are simultaneously excited, *i.e.* two or more reciprocal lattice points lie simultaneously on the Ewald sphere. Figure 1 demonstrates the geometry of multiple diffraction. *O* is the origin of the reciprocal lattice, *C* is the center of the Ewald sphere and the circle shown here is the intersection of this plane with the Ewald sphere. k_o represents the direction of the incident beam and k_h and k_p represent the direction of reflected beams. The diffraction vector *OP* lies in the plane while *OH* lies out of the plane. When the crystal rotates around the primary vector *OP* (the so called ψ scan), the reciprocal lattice point *H* may also touch the surface of the Ewald sphere. When it happens, the reflected beam k_h by the diffraction wave vector *OH* can also serve as a primary beam for diffraction wave vector *HP*, letting another diffraction beam be excited in the same direction of k_p hence resulting in the redistribution of the total amount of intensity. Strictly speaking, multiple diffraction has two effects: if the primary reflection **P** (also called main reflection, hereafter a single bold letter is used to indicate the reflection throughout this paper) is a forbidden or weak reflection and both the second excited reflection **H** (called simultaneous or operative reflection) and the corresponding **P-H** (called coupling or cooperative reflection) are strong, the intensity of the primary reflection will be enhanced, such effect is the so called *Umweganregung*; On the other hand, if **P** is a strong reflection and both **H** and **P-H** are weak, its intensity will decrease which is defined as *Aufhellung*. Our interest in multiple diffraction is restricted to *Umweganregung* in the case of weak reflections.

For quasicrystals, multiple diffraction is unavoidable when collecting large data sets owing to the infinite and dense reciprocal lattice points. It is expected to seriously influence weak Bragg intensities, which are crucial for the determination of their structures and the poor fit of weak reflections during structure refinement has once been attributed to the effect of multiple diffraction (Takakura *et. al.*,

2. Experimental and Data Processing

The composition of the sample is $\text{Al}_{72.5}\text{Co}_{18.5}\text{Ni}_9$ and its detailed preparation procedure can be found elsewhere (Strutz, *et. al.* 2009). The size of the samples used for the in-house and synchrotron radiation measurements was about $100\ \mu\text{m}$ and $20\ \mu\text{m}$ respectively. The in-house measurements have been performed with a four-circle diffractometer equipped with a CCD (Xcalibur, Oxford Diffraction, 50 kV, 40 mA, graphite monochromatized $\text{MoK}\alpha$ radiation). The synchrotron radiation (SR) were carried out at the Swiss-Norwegian beamlines (SNBL, BM01A) at ESRF, Grenoble. This bending-magnet beamline was installed for parallel-beam optics - that is a double Si(111) monochromator. The wavelength of the monochromatic beam was tuned to be $\lambda = 0.7000\ \text{\AA}$ with a energy resolution of $\delta\lambda/\lambda \approx 1.4 \times 10^{-4}$.

Two individual MD events are measured by performing ψ - ω -scans as described before (Fan *et. al.* 2011) in-house to estimate the maximum amplitude that the reflected intensity of some weak reflections can reach when affected by multiple diffraction. A wide range of ψ scan has been carried out with SR in order to estimate the occurring frequency of MD events. In-house, two main reflections, $\mathbf{P}_1 = (2\ 1\ 0\ 1\ 0)$ and $\mathbf{P}_2 = (\bar{1}\ 1\ 0\ 1\ 0)$, were selected from the 20 equivalent reflections of $(2\ 1\ 2\ 1\ 0)$ by adding two strong reflections $(1\ 1\ 1\ 1\ 0)$ and $(1\ 0\ 1\ 0\ 0)$. The MD event is expected to occur in a range of 0.2° (the FWHM is 0.1°) on account of the beam divergence and crystal perfection by some pilot measurements, so the step size of ψ scan is set to be 0.01° . To compensate small mis-alignment of the sample, at each step of ψ , an ω scan (11 steps, in total 0.1°) was performed around the theoretical ω value. The exposure time was set to be 30 s per ω - ψ step to get reliable intensity I of the main reflection during the ω - ψ scan. When $\mathbf{H}_1 = (1\ 0\ \bar{1}\ 0\ 0)$ and $\mathbf{H}_2 = (\bar{1}\ 0\ 0\ 1\ 0)$ serve as operating reflections for \mathbf{P}_1 and \mathbf{P}_2 , one of their excited value of ψ are predicted to be 10.90° and 2.45° , respectively. These operating reflections are considered to be excited when its length satisfies $|k_h| \leq (1.0 \pm 0.05\%) 1/\lambda$. All these calculations are based on the geometry of 4-circle kappa diffractometer and Azimuthal angles as described in detail by Meyer (1998), which are carried out by a self-written program. Although theoretically a operating reflection will be excited at least 2 times if carrying out 360° ψ -scans, restricted by the geometry of the 4-circle diffractometer, it's impossible to measure each corresponding MD event. At SNBL/ESRF Grenoble, the high flux of the beam allowed the measurement of a wide ψ -scan from 0 to 40° with a step size of 0.01° for $\mathbf{P}_2 = (\bar{1}\ 1\ 0\ 1\ 0)$. At each step of ψ , a 0.5° ω scan has been carried out. A small program has been developed to read out the pixel counts by applying a circle mask on the frame at each step.

For a full data set, all data collection and data processing were performed using the software package CrysAlisPro (Oxford Diffraction, 2009). It need to emphasize that the three dimensional lattice parameters used to index the data sets are $a=3.9888(12)\ \text{\AA}$, $b=3.9891(11)\ \text{\AA}$, $c=4.0645(11)\ \text{\AA}$ and $\alpha=90.01(2)^\circ$, $\beta=90.00(2)^\circ$, $\gamma=107.99(3)^\circ$ in the BL-scheme (Busing & Levy (1967)), which is equivalent to $a_{1-4}=3.989\ \text{\AA}$, $a_5=4.065\ \text{\AA}$ in S-scheme (Steurer, 2004), as well as $a_{1-4}=2.884\ \text{\AA}$ and $a_5=4.065\ \text{\AA}$ by the five-dimensional description in the YI-scheme (Ishihara and Yamamoto, 1988). In this article, the S-scheme is used to index the data sets and to describe the ψ -scans of multiple diffraction measurements for its convenience and the YI-scheme is used only to describe the average structure model. The transform matrix for the indices from S-scheme to the YI-scheme is:

$$\mathbf{T}_{S \rightarrow YI} = \begin{pmatrix} 0 & 1 & 0 & \bar{1} & 0 \\ 0 & 1 & 1 & \bar{1} & 0 \\ \bar{1} & 1 & 1 & 0 & 0 \\ \bar{1} & 0 & 1 & 0 & 0 \\ 0 & 0 & 0 & 0 & 1 \end{pmatrix} \quad (1)$$

It was found that the integration is very sensitive to lattice parameters. To distinguish the uncertainties of integrated intensities introduced by the data processing and those introduced by MD effects, 10 cycles of integration have been repeated to check the robustness of the integration procedure. In these 10 cycles of integration, the output lattice parameters were directly used for the following

cycle. At last the median value of 10 integrated intensities (before absorption correction and outlier rejection) for each reflection has been used when checking the MD effects.

It is found that the lattice parameters are quite stable during these 10 cycles of integration: the maximum variance of these 6 lattice parameters is 0.022%. There are 17332 reflections (the physical and perpendicular resolutions are 1.60 \AA^{-1} and 1.50 \AA^{-1} respectively) in total. Among them, there are 608 reflections with a larger standard deviation of integration than that of counting statistics, *i.e.*, the values output by the CrysAlisPro package. These 608 reflections including both strong and weak reflections, thus special attention will be paid to them when checking the MD events in this data set later on.

3. Theoretical Background

3.1. Simulation of ψ -Scan Measurements

3.1.1. Simple Approach

The algorithm used here is similar to that developed in our previous work (Fan *et al.* 2011). Assuming that the structure factor of the primary reflection is very weak compared to those of operating and cooperating reflections and that the Lorenz and polarization factors are neglected, the intensity change ΔI_{prim} is given by (Rossmann, 1986):

$$\Delta I_{prim} = \rho \cdot \sum_{op,coop} (|F_{op}| \cdot |F_{coop}|)^2 \quad (2)$$

where ρ is a coefficient; F_{op} and F_{coop} are the structure factors for the operative and cooperative reflections respectively; The summation runs over all the involved operative and cooperative reflections. The purpose of such simulation is to check out if the algorithm is sufficient and reliable to predict the observed MD peaks in a semi-quantitative way. In all calculations, the following aspects were considered for comparison with experimental results: (a) a reflection is considered to be *strong* compared to another reflection if its intensity is more than 100 times larger, and a reflection is considered to be *weak* to another if its intensity is less than 0.01 times of the latter. (b) The Bragg reflections list is generated by five Miller indices $hklmn$, with maximum and minimum value 8 and -8 respectively, and the length of each selected diffraction vector in the physical and perpendicular space is less than 1.60 \AA^{-1} and 1.70 \AA^{-1} respectively. In total, there are 52,663 reflections. (c) The coefficient ρ in Equation (2) was calculated to be 5.2×10^{-9} and 6.8×10^{-9} using expression (2) by the observed SR *umweganregung* peaks A and B (see Figure 2) and the integrated intensities of involved reflections, respectively. (Take peak A as an example, as the reflected intensity changes from 205 to 256, see Figure 2 (a), so $\Delta I_{prim}/I_{prim} = 25\%$. From the integration results, the integrated intensities of the main, operative and cooperative reflections of peak A are $7(1) \times 10^2$, $3.0(1) \times 10^5$ and $1.12(3) \times 10^5$, respectively. Using expression (2), one can easily get $\rho = 5.2 \times 10^{-9}$. Note that the integrated intensity of strongest reflection in the full data set, (0 1 1 1 1), in the data set is not available owing to the limited dynamic range of the CCD.) It need to emphasize that the summation of pixel counts deeply depends on the center and size of the mask. It has been tested that for peak A, $\Delta I_{prim}/I_{prim}$ may change from 25% to 50% when the center of the mask changes. In this case, the coefficient ρ in Equation (2) will double to 5.2×10^{-9} . The in-house observed *umweganregung* peaks (see Figure 3) have also been used to crosscheck the reliability of the coefficient ρ , which result in $\rho \approx 1.5 \times 10^{-8}$. Finally, the coefficient ρ in Equation (2) was determined to be $\rho = 1.5 \times 10^{-8}$, *i. e.*, the upper limit of all these calculated values, in the purpose of not missing any significant *umweganregung* peak in the simulation. (d) To decide whether a reflection is simultaneously excited or not when performing a ψ -scan, the Ewald sphere can be regarded as two limiting spheres, with radius $1/(\lambda - \Delta\lambda)$ and $1/(\lambda + \Delta\lambda)$. And considering this, the thickness of the Ewald sphere is set to be $0.05\% \cdot (1/\lambda)$. There are 155,806 reflections included in the calculation as some reflections may appear several times owing to the assumed thickness of Ewald sphere. (e) When one reflection is excited at several steps (the step size is 0.01°), its absolute structure factor are assumed to reach maximum value at the median step and be equally distributed among other steps.

All the theoretical structure factors are calculated by the average structure model for the basic Co-rich decagonal Al-Co-Ni quasicrystal (See Strutz, *et. al.* 2009) and its ideal version before refinement was used. The R value are $wR=24.4\%$ and $R=30.9\%$ for 811 unique reflections based on one full collected data set with unit weighting scheme, *i. e.*, $\sqrt{\frac{\sum(F_{obs}-F_{cal})^2}{\sum F_{obs}^2}}=24.4\%$, where summation runs over all the unique reflections. As its value is dominated by strong reflections, implying the calculated structure factors are reliable for strong reflections.

To estimate the reliability of the idealized model, the integrated intensities themselves are used as the unit weight, which result in $R=8.3\%$ based on the same data set, *i. e.*, $\sum_i(I_{obs} - I_{cal}) / \sum_i I_{obs}=8.3\%$, where i runs over all unique reflections. It can be deduced that the maximum uncertainty of $(|F_{op}| \cdot |F_{coop}|)^2$ in expression (2) is $2 \times 8.3 = 16.6\%$, implying that the ideal model is quite reliable.

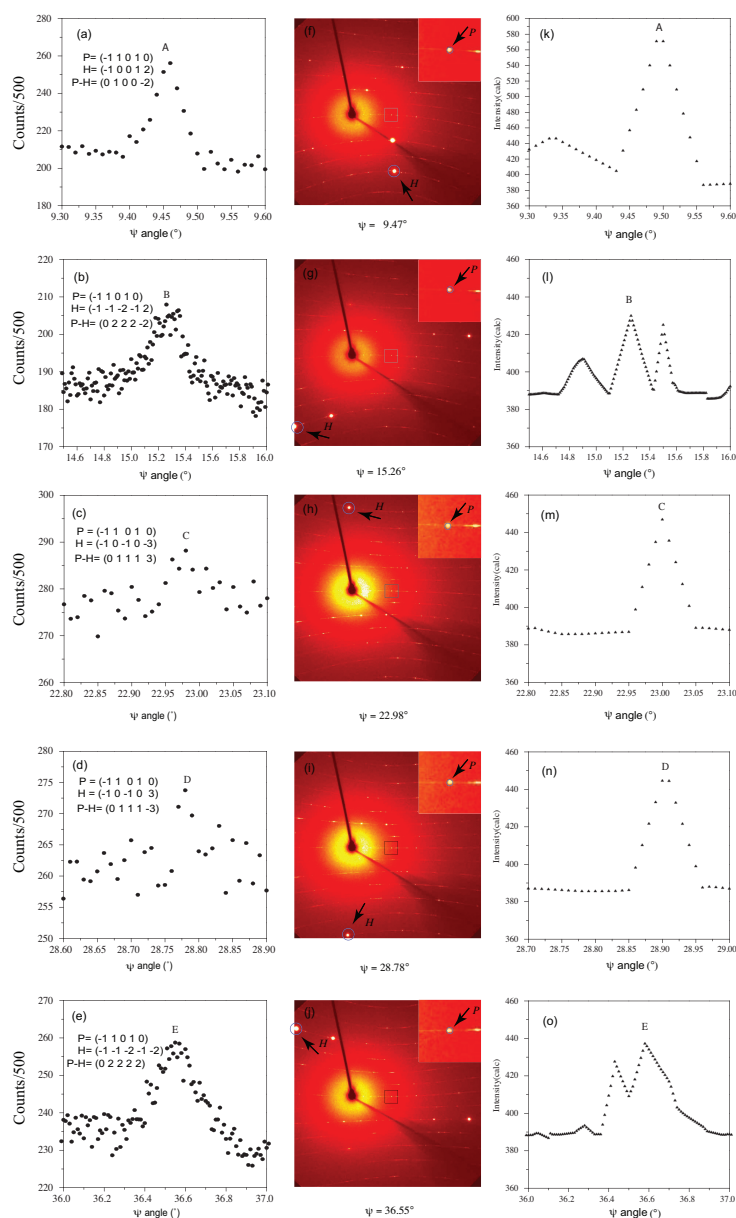


Figure 2. Significant multiple diffraction peaks of primary reflection $(-1\ 1\ 0\ 1\ 0)$ during a 40° of ψ -scans. From the measurements, these peaks are located at (a) 9.47° (peak A), (b) 15.26° (peak B), (c) 22.98° (peak C), (d) 28.78° (peak D), and (e) 36.55° (peak E); From the simulation by the simple approach introduced in the text, they are located at (k) 9.495° (peak A), (l) 15.26° (peak B), (m) 23.00° (peak C), (n) 28.905° (peak D), and (o) 36.58° (peak E). Figure (f)-(j) demonstrates the appearance of corresponding main and operating reflections on the diffraction frames. The marked zones that contain the main reflection are shown enlarged in the insert figures.

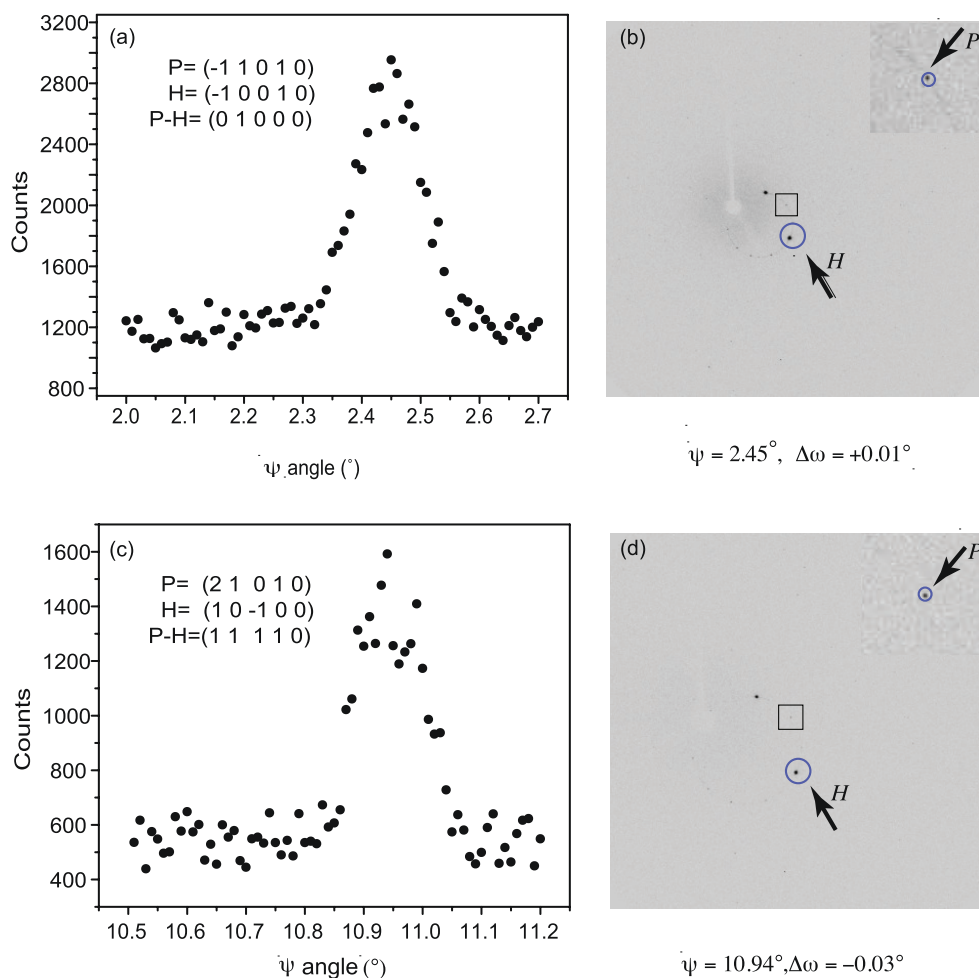


Figure 3. Intensity of a weak reflection as a function of the azimuthal angle. At the peak, the main contributing simultaneous reflection is (a) $\mathbf{H} = (\bar{1}\ 0\ 1\ 0\ 0)$ and (c) $\mathbf{H} = (1\ 0\ \bar{1}\ 0\ 0)$. The relative positions of the involved reflections at the peak are shown by CCD images right to them, (b) and (d) respectively.

3.1.2. Complicated Approach

As we will see, all the significant MD events can be predicted by the simple approach. However, it does not consider the polarization and the Lorenz effect, nor the size of the sample, the beam divergence, wave length spread and mosaic spread. In order to check its reliability, a bottom-up complicated approach has been applied to simulate the ψ -scans diffraction pattern. By modifying the UMWEG program (Rossmannith 2003) which can simulate the MD patterns of periodic crystals, now it is also applicable to quasicrystals as well. In the modified version, the structure factors and their phases are calculated from the mentioned ideal average structure model of basic Co-rich decagonal Al-Co-Ni. The absorption effect has been neglected by setting the coefficients of absorption to be 1.0. The polarization of the beam is 95% in the horizontal plane and 5% in the vertical diffracting plane. Similar to that of traditional crystals, the peak width of ψ -scan diffraction pattern of quasicrystals depend on the radius r of the sample, the wavelength spread $\Delta\lambda/\lambda$, the beam divergence δ and the mosaic spread η . The exact expression could be found elsewhere (Rossmannith 2007). The individual contributions of these parameters to the FWHM have been intensively tested. Owing to the uncertainties of measurement and summation of pixel counts, the actual FWHM should be larger than 0.05° , as deduced from peak C. However, it should be less than 0.2° suggested by peak B and peak D because they are attributed to several individual peaks, as we will see later. It is found that when the radius of the mosaic block less than $1000\ \text{\AA}$, *i.e.*, ε greater than 0.001, its contribution to the FWHM is more than 0.2° . Therefore, ε should be less than 0.001. It has also been calculated that when the mosaic spread η equals to 0.1° , its contribution to the FWHM is 0.12° . In the present simulations, $\varepsilon = 0.0007$ and the mosaic spread $\eta =$

0.01° were used. The beam divergency $\delta = 0.00143^\circ$ and $\Delta\lambda/\lambda = 1.4 \times 10^{-4}$ adopted by Thorkildsen *et. al* (2005) were used as well. The FWHM is calculated to be less than 0.17° by these parameters.

3.2. Simulation of MD Events in a Collected Full Data Set

Theoretically, one can collect a data set of a quasicrystal by performing one or several ψ -scan measurements for several reflections. However, in practice, the most popular strategy is to collect by combining several runs with special angle setting. On the one hand, it adds the complexity of the simulation of MD events as there is no available approach to simulate the MD events during ω scans. On the other hand, it provides another way of extracting weak reflections which may be significantly affected by MD effects from the full data set. From integration results, one know the maximum integrated intensity of each reflection appear on a certain diffraction frame. It's well know that the profiles of some strong reflections may span over several diffraction frames, which implying that they may affect weak reflections on several diffraction frames. However, by checking some selected strong reflections, the profiles of these strong reflections are very sharp and the integrated intensities reduce at least 50% in the neighboring two diffraction frames to the one has the maximum integrated intensity (the oscillation angle of ω -scans is 0.2°). Therefore, it's sufficient to consider those reflections appear simultaneously on the same as well as on the neighboring two diffraction frames when simulate MD events. As demonstrated in the following section, the simple approach introduced above is sufficient and quite reliable to predict significant MD events. Thus one can also apply it to determine the significant MD events in the collected full data set. The difference is that according to the integration resulting file, the whole involved reflections are already available and there is no necessary to predict when these reflections touch the Ewald sphere. In case of missing some significant MD events, the coefficient $\rho = 1.5 \times 10^{-8}$ has also been adopted. The summation runs over all the operating reflections which have theoretical intensities 100 times of that of the main reflection in the neighboring two diffraction frames and the corresponding cooperative reflections. All the theoretical structure factors are calculated by the average structure model as well.

4. Results and Discussion

4.1. ψ -Scan Multiple Diffraction Pattern

Figure 3 (a) and (c) shows some results of in-house ψ -scans measurement. Significant multiple diffraction peaks are observed where expected, with only a small bias of the theoretical angle setting. Each black point represents the maximum of the 11 step ω scan. According to the CCD frames, in both cases two strong simultaneous reflections appear, (Figure 3(b) and (d)), but only one of them contributes mainly to the observed peaks as the intensity of the cooperating reflection corresponding to the other simultaneous reflection is weak. The positions of the primary reflections and main contributing simultaneous reflections are indicated by arrows. From Figure 3 (a) and (c), one can see that the maximum value of the intensity is about 3 times of the original intensity. The enhancement seems smaller than that reported by Eisenhower *et. al.* (1998) for a similar decagonal quasicrystal $\text{Al}_{72.5}\text{Co}_{16.5}\text{Ni}_{11}$. It may be attributed to the large wavelength ($\lambda=1.63 \text{ \AA}$) used in their experiments by synchrotron radiation, resulting in the area of the Ewald sphere in the present situation is 5.42 times of theirs. More reflections are included in the interaction, which may remove some energy from the strong operating and cooperating reflection. Indeed, many weak reflections except the primary reflection can be clearly seen on the CCD images. Note that the primary reflections ($\bar{1} 1 0 1 0$) and ($2 1 0 1 0$) on Figure 3(a) and (c) respectively are equivalent reflections. The measured intensity should have comparable intensities. However, the intensity of the latter is obviously smaller than the former, it is because during the measurement for the reflection ($2 1 0 1 0$), the distance of the CCD detector was set to 100 mm by accident instead of 60 mm by default.

Figure 4(a) shows the 40° of ψ -scans of one primary reflection ($\bar{1} 1 0 1 0$). The step size of the ψ -scan is 0.01°. At each specific ψ angle, an ω scan with width of 0.5° was performed. The value of ω was calculated by the the known orientation matrix and the standard angle setting at $\psi=0$. The

counts show vertically are integrated around the center of the reciprocal point of vector $(\bar{1} 1 0 1 0)$ by applying a mask with a radius of 5 *pixels*. The jump of the intensity around 22° is caused by the refilling electrons of the storage ring. Five peaks can be clearly seen in Figure 4(a). All these 5 peaks are reproduced by simulation as shown in Figure 4(b) by the simple approach. The operating and cooperating reflections and the corresponding theoretical intensities of these peaks are listed in Table 1.

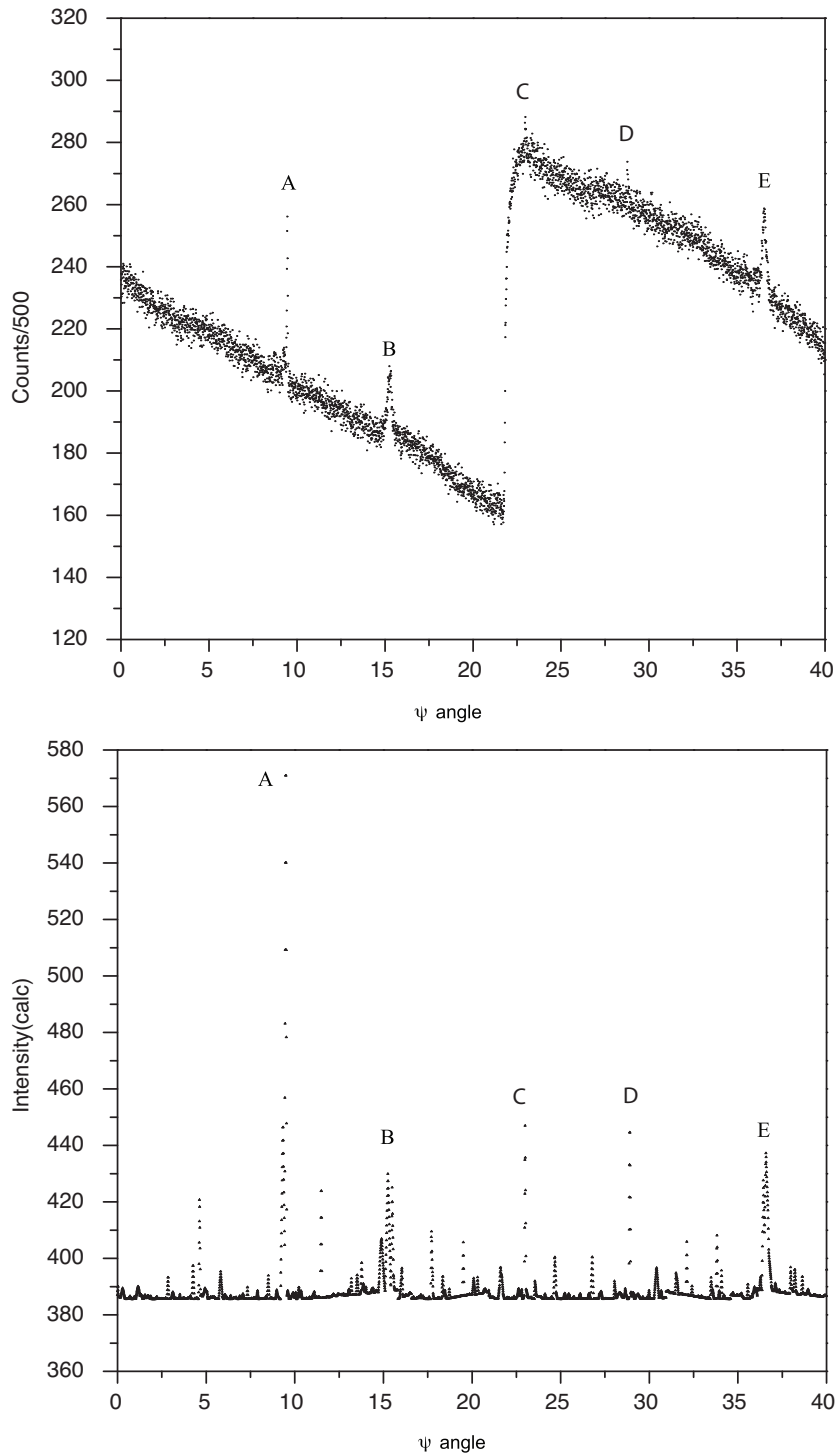


Figure 4. Intensity variation of primary reflection $(\bar{1} 1 0 1 0)$ during a 40° of ψ -scans, (a) experimental measurements and (b) simulation results by the simple approach.

Table 1. The main contributing strong operating and cooperating reflections of the MD peaks during the 40° ψ scans around primary reflection ($\bar{1}1010$), the theoretical intensity of the main reflection is 385.6

Peaks	ψ	H	P-H	I_{calc}^P ($\times 10^5$)	I_{calc}^{P-H} ($\times 10^5$)	ΔI_{prim}^H	ΔI_{prim}^{tot}	$\frac{\Delta I_{prim}^{tot}}{I_{prim}}$ (%)
A	9.49	($\bar{1}0012$)	(0100 $\bar{2}$)	1.97	0.63	185.3	185.4	48.1
B	15.26	($\bar{1}\bar{1}\bar{2}\bar{1}2$)	(0222 $\bar{2}$)	0.17	0.12	36.6	44.4	11.5
C	23.00	($\bar{1}0\bar{1}0\bar{3}$)	(01113)	0.15	2.59	58.6	61.4	15.9
D	28.90	($\bar{1}0\bar{1}03$)	(0111 $\bar{3}$)	0.15	2.59	58.6	59.0	15.3
E	36.58	($\bar{1}\bar{1}\bar{2}\bar{1}\bar{2}$)	(02222)	1.97	0.12	36.6	51.6	13.4

Note that peak A is the strongest of the 5 peaks because of both its operating and cooperating reflections are strong reflections and the product of their intensities has the largest value. The intensity variation of peak B and E, C and D are the same and the diffraction pattern is symmetric at ψ angle 25.92° . From the simulation, one can easily find that it is caused by the symmetry of the related operating and cooperating reflections. From the ψ -scans measurements and the semi-quantitative simulation results, we may conclude that only a small number of reflections are affected by multiple diffraction. For example, by simulation, for the primary reflections ($\bar{1}1010$) there are 72 of 4,000 positions (40° , step size 0.01°) whose intensity is enhanced by 10%, *i.e.*, from 385.6 to 424.2. Figure 4(a) also suggests that most affected positions are saturated in the background.

In order to crosscheck the reliability of the simple approach, the bottom-up complicated approach has been applied to simulate the ψ -scans diffraction pattern and to check out if the peaks are really caused by those operating and cooperating reflections listed in Table 2. It need to emphasize that all the experimental measurements are performed after refining the instrument model. From the refined instrument model, we know that the primary beam is misaligned 0.81° . This parameter is very important in simulating the position of MD peaks as such offset was not considered by UMWEG. Figure 5 shows the simulated and measured diffraction pattern after correction of the 0.81° of ψ -shift. The enlarged parts of peak A and peak E are shown in Figure 6 and Figure 7, respectively. From these 3 figures, it is obvious that peak A, peak B and peak E are all caused by the overlay of several MD peaks and there is a mirror at 25.91° . At the theoretical positions of peak C and D, there are no other strong MD peaks around. It is confirmed that the contributing operating reflections of these 5 peaks are exactly the same as predicted by the simple approach as shown in Table 3. Therefore, the quantitatively results suggest that the qualitative results are also very reliable as the five peaks can be found successfully as well.

Table 2. Some weak reflections significantly affected by MD effects during collecting the full data set and their main contributing operating and cooperating reflections.

(run, frame)	P	H	P-H	I_{Prim}	σ_{prim}	ΔI_{prim}^{tot}	I_{median}
(1,215)	(14421)	(01101)	(13320)	724.7	77.4	393.4	379.9
(1,540)	($\bar{1}1\bar{1}03$)	(00002)	($\bar{1}\bar{1}\bar{1}01$)	1467.8	69.6	126.8	1259.1
(2,195)	(21116)	(00012)	(21104)	683.2	73.6	86.1	506.8
(2,254)	($\bar{1}0\bar{2}\bar{1}4$)	($\bar{1}0\bar{1}01$)	(00 $\bar{1}\bar{1}3$)	498.0	59.6	165.4	197.7
(2,332)	($\bar{1}\bar{1}012$)	(0 $\bar{1}0\bar{1}2$)	(100 $\bar{2}0$)	891.8	57.5	325.2	563.5
(2,549)	($\bar{1}0\bar{1}00$)	(00 $\bar{1}00$)	($\bar{1}0000$)	1606.8	30.8	194.9	1357.6
(2,593)	($\bar{1}2220$)	($\bar{1}22\bar{1}0$)	(000 $\bar{1}0$)	486.9	45.3	161.4	351.6
(2,664)	($\bar{1}\bar{1}000$)	(0 $\bar{1}012$)	($\bar{1}00\bar{1}2$)	5930.7	59.4	204.4	2811.9

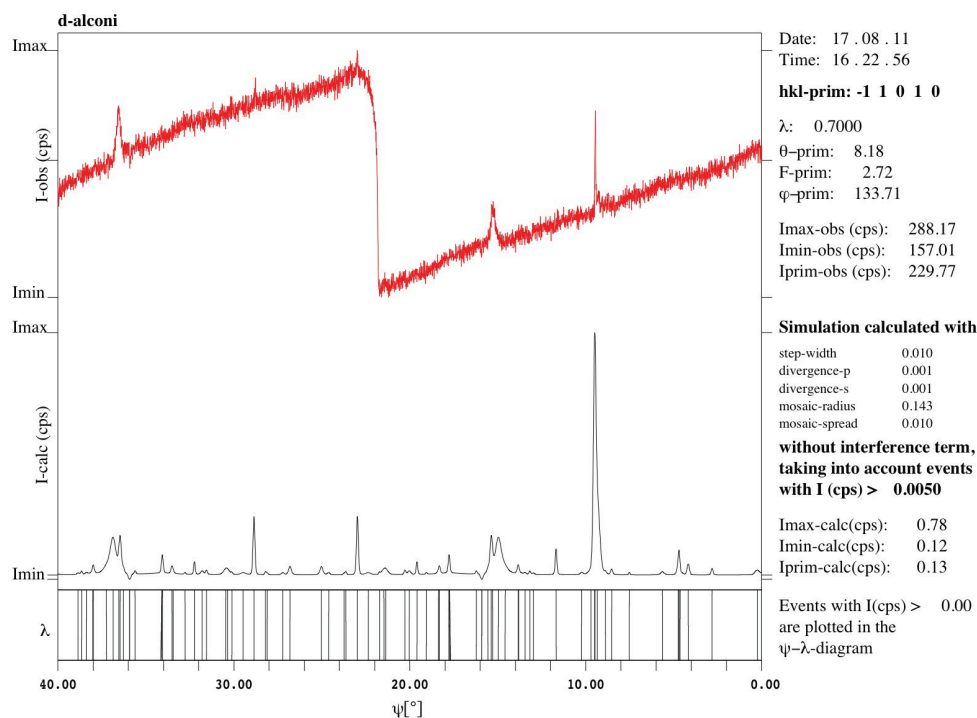


Figure 5. Simulated ψ -scans without considering the interference term and including the ψ - λ diagrams. The measured ψ -scans are included and A 0.81° ψ -shift has been corrected according to the refined instrument model .

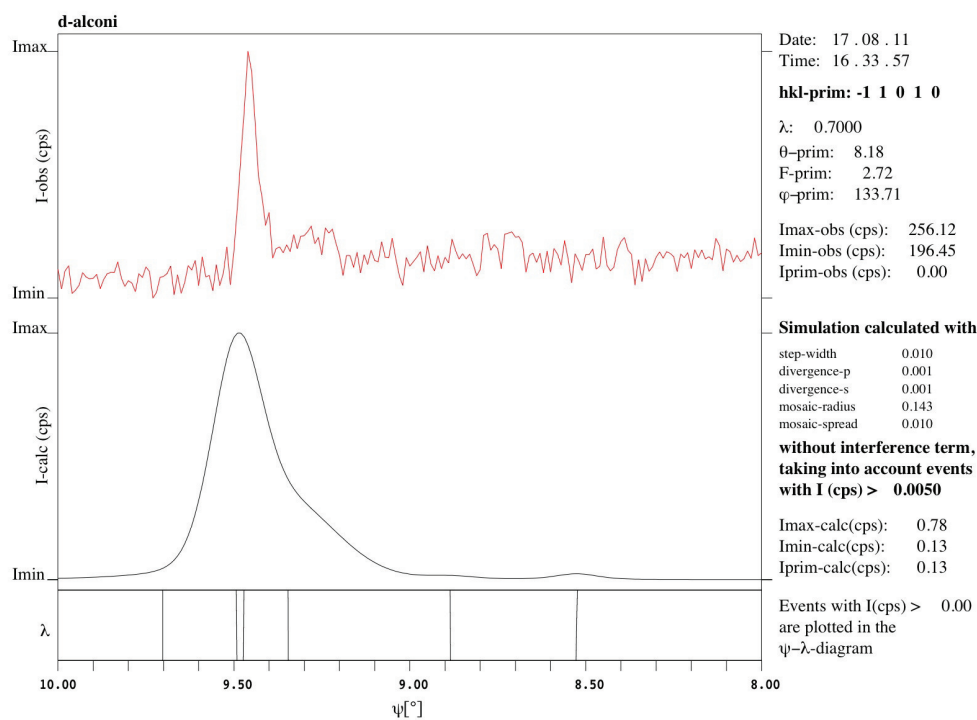


Figure 6. Enlarged peak A of the simulated ψ -scans without considering the interference term and including the ψ - λ diagrams. It is mainly composed of 3 individual MD peaks locating at 9.346° , 9.473° and 9.492° . The maximum of the peak locates at 9.492°

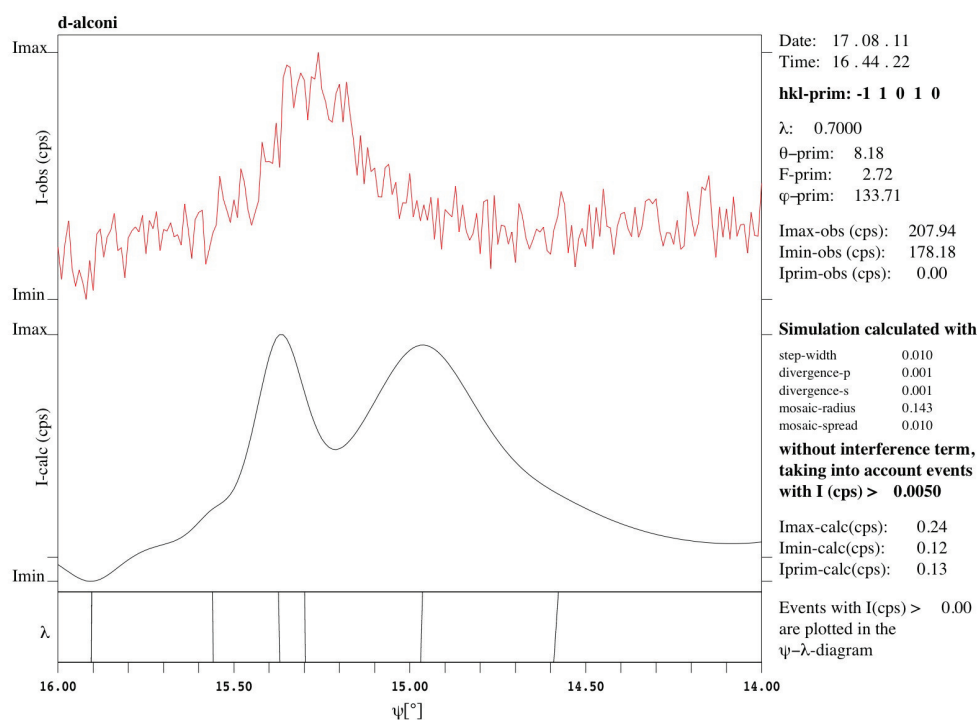


Figure 7. Enlarged peak B of simulated ψ -scans without considering the interference term and including the ψ - λ diagrams. It is mainly composed of 4 individual MD peaks locating at 14.967° , 15.298° , 15.371° and 15.560° . The maximum of the peak locates at 14.967°

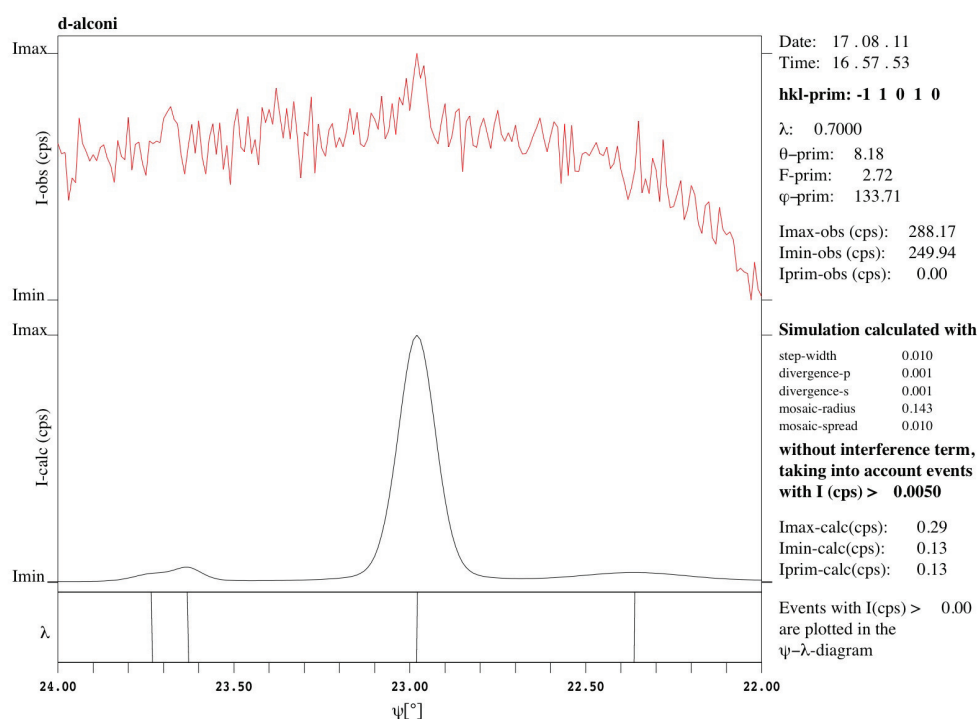


Figure 8. Enlarged peak C of simulated ψ -scans without considering the interference term and including the ψ - λ diagrams. It is mainly attributed to a single MD peak locating at 22.980° .

4.2. Effect of Multiple Diffraction on the Quality of the one Full Data Set

From the simulation results by the simple and the complicated approaches, it suggests that although the simple approach based on a simple assumption, it is still sufficient and reliable to

predict significant MD events. The latter is of vital importance when evaluating the MD effects to the diffraction data quality of quasicrystals. By the most pessimistic assumptions discussed in section 3.2, one can figure out all the candidate weak reflections that could be potentially affected by MD effects when collecting the full data set. These weak reflections are selected when satisfy:

$$\Delta I_{prim} > \sigma_{prim} \quad (3)$$

and

$$I_{prim} - I_{median} > z_{max} \cdot \sigma_{prim} \quad (4)$$

where ΔI_{prim} is the amount of enhanced intensity calculated by expression (2), I_{prim} and σ_{prim} are the integrated intensity and its corresponding standard deviation of a primary reflection, respectively. I_{median} is the median value of integrated intensity of all the equivalent reflections including the primary reflection. Both values of 1 and 2 have been tested for z_{max} , however, it is found that $z_{max}=2$ is more reasonable. It need to note that these weak reflections that contaminated by MD effects cannot be automatically rejected before empirical absorption fitting as the default value is $z_{max}=12$ (Blessing, 1997).

It is finally found that there are only 22 candidate of weak reflections among 17332 reflections that satisfy both expressions (3) and (4) during collecting the full data set. When comparing them with their equivalent reflections before and after absorption and outlier rejection, it is found that only 7 and 8 reflections respectively have the maximum integrated intensities among their equivalent reflections which strongly suggests that they are affected by MD effects. There are some weak reflections that satisfy the criteria, but they does not have the maximum integrated intensity among their equivalent reflections, implying the MD effect is not the only source of strengthening weak reflections. The effect of these 10 reflections to the diffraction data quality of the whole data set can be evaluated by the widespread statistic factor:

$$R_{merge} = \frac{\sum_H \sum_i |I_i(H) - \overline{I_H}|}{\sum_H \sum_i |I_i(H)|} \quad (5)$$

Here, $I_i(H)$ means the intensity of an individual reflection and $\overline{I_H}$ means the average intensity of a group of equivalent reflections labelled by i . The summation runs over the whole reflections and please note that 10/*mmm* Laue group is applied to check the equivalent reflections and only those reflections with redundancy no less than 3 are considered in the present calculation. it's not surprising that the change of R_{merge} is negligible when rejecting these 22 reflections.

The 8 reflections that satisfy expressions (3) and (4) and have the maximum integrated intensities among their equivalent reflections are listed in Table 4 with their main contributing operating and cooperating reflections. In most cases, not only one operating reflection strengthen the main reflection and the operating reflection does not have to on the same frame as the main reflection. For instance, although the operating reflection (01101) on frame (1, 215) contribute 272.8 of the total MD effect 393.4 (69.3%), there is another operating reflection (13311) on frame (1, 217) also contribute 105.7. On the other hand, even there are several strong operating reflections appear on the same diffraction frame as the main reflection, if the operating and cooperating reflections are not both strong, they still contribute little MD effect. *e.g.*, there are two strong operating reflections ($\bar{1}\bar{1}\bar{1}\bar{1}0$) and (00 $\bar{1}$ 00) on frame (2, 549), but only the latter contribute mainly to the MD effect (93.6%).

Finally, let's check the MD effects on the structure refinement of quasicrystals. It is found that the calculated structure factors are larger than the observed ones for the equivalent reflections of 5 out of these 12 reflections, suggesting that MD effect is not the main reason for the poor fit of weak reflections in the refinement of quasicrystals where the observed structure factors are always larger than the calculated ones.

5. Conclusions

Multiple diffraction effects can significantly strength the intensity of the weak reflections in a basic Co-rich decagonal Al-Co-Ni quasicrystal as well as in *i*-quasicrystal as demonstrated by in-house and synchrotron radiation ψ -scans measurements. By comparing simulation results of MD peaks and observed ψ scan diffraction patterns, it reveals that a simple version of kinematical diffraction theory is sufficient and reliable to predict significant MD events. For the first time, the MD events in a complete collected data set have been investigated and the results suggest that its occurring frequency is quite low. The intensities of weak reflections themselves that affected by MD effects maybe very significant (satisfy the proposed criteria expressions (4) and (5)), however, their effects to the diffraction data quality is negligible after absorption correction and averaging of equivalent reflections. It's also confirmed that MD effect is not responsible for the poor fit of weak reflections in the refinement of quasicrystals. The present work supports the previous idea that the number of reflections so strongly affected by the MD effect is not large enough to explain the typical bias for some weak reflection (Kuczera,*et. al.* 2012).

Funding: This research was funded by the National Natural Science Foundation of China(Grant Nos. 52173231 and U23A20537) as well as the Swiss National Science Foundation under Grant SNF200020-121568.

Data Availability Statement: Data supporting reported results are available upon reasonable request.

Acknowledgments: The author is indebted to Walter Steurer who initiated the project on the effect of multiple diffraction during refinement of quasicrystal structures more than 15 years ago. The author also gratefully acknowledge Angelica Strutz for providing the sample and the ideal average structure model and Thomas Weber, Elizabeth Rossmannith and Arkadiy Simonov for useful discussions during those time. The staff of the Swiss-Norwegian beamline (SNBL) at ESRF is acknowledged for the beamline time provided

Conflicts of Interest: The authors declare no conflicts of interest.

Abbreviations

The following abbreviations are used in this manuscript:

MD	Multiple diffraction
SR	Synchrotron radiation
SXRD	Single crystal X-ray diffraction

References

- Blessing, R. (1997). Outlier treatment in data merging. *J. Appl. Cryst* 30,421-426.
- Buganski I., Strzalka R. & Wolny J. (2019). Phason-flips refinement of and multiple-scattering correction for the d-AlCuRh quasicrystal.*Acta. Cryst* A75,352-361.
- Buganski I., Strzalka R. & Wolny J. (2020). A new approach to phason disorder for a decagonal quasicrystal: the moment series expansion of the tiling distribution function for AlCuRh.*J. Appl. Cryst* 53,904-913.
- Buganski I. & Bindi L. (2021). Insight into the structure of decagonite – the extraterrestrial decagonal quasicrystal.*IUCrj* 8,87-101.
- Buganski I., Strzalka R. & Wolny J. (2024). The physical space model of the Tsai-type quasi-crystal.*Acta. Cryst* B80,1-10.
- Busing, W. & Levy, H. (1967). Angle calculations for 3-and 4-circle X-ray and neutron diffractometers. *Acta. Cryst* 22,457-464.
- Fan, C. Z.,Weber, Th., Deloudi, S. & Steurer, W. (2011). Multiple diffraction in an icosahedral Al-Cu-Fe quasicrystal. *Phil. Mag.*, 19-21, 2528-2535.
- Giacovazzo, C., Monaco, H. L., Viterbo, D., Scordari, F., Gilli, G., Zanotti, G. & Catti, M. (1992) *Fundamentals of crystallography*
- Kuczera, P., Wolny J. & Steurer W. (2012). Comparative structural study of decagonal quasicrystals in the systems Al–Cu–Me (Me = Co, Rh, Ir).*Acta. Cryst* B68,578-589.
- Ishihara, K & Yamamoto, A. (1988). Penrose patterns and related structures. I. Superstructure and generalized Penrose patterns. *Acta. Cryst* A44,508-516.

11. Meyer, M. (1998). *Construction of a multi-purpose X-ray CCD detector and its implementation on a 4-circle kappa goniometer* [PhD. Thesis , EPFL, Lausanne]
22. Rossmannith, E. (1986). Comparison of an Umweganregung pattern, measured on an automatic single-crystal diffractometer, with calculated patterns. *Acta. Cryst. A* 42,344-348.
22. Rossmannith, E. (2003). UMWEG: a program for the calculation and graphical representation of multiple-diffraction patterns. *J. Appl. Cryst* 36,1467.
22. Strutz, A., Yamamoto, A. & Steurer W. (2009). Basic Co-rich decagonal Al-Co-Ni: Average structure. *Physical Review B*, 80, 184102.
22. Strutz, A., Yamamoto, A. & Steurer W. (2009). Basic Co-rich decagonal Al-Co-Ni: superstructure. *Physical Review B*, 82, 064107.
22. Strzalka R., Buganski I., Kuczera P., Pytlik L. & Wolny J. (2019) Atomic Structure of Decagonal Al-Cu-Rh Quasicrystal–Revisited.*Crystals* 9,78.
22. Steurer W. (2004). Twenty years of structure research on quasicrystals. Part I. Pentagonal, octagonal, decagonal and dodecagonal quasicrystals. *Z. Kristallogr* 219,391-446.
22. Steurer W. (2017). Quasicrystal structure and growth models: discussion of the status quo and the still open questions.*Journal of Physics: Conf. Series* 809,012001.
22. Takakura, H., Gómez, C. P., Yamamoto, A., De Bossieu, M. & Tsai, A. P. (2007) . Atomic structure of the binary icosahedral Yb–Cd quasicrystal. *Nature mater.*, 6, 58-63.
22. Takakura, H. & Mizuno, R. (2015). Multiple Diffraction in an Icosahedral Al-Cu-Rh Quasicrystal: X-Ray Experiment and Simulation. *Mater. Struct.* 22, 281.
22. Thorkildsen, G., Mathiesen R. H. & Larsen H. B. (1999). Angle calculations for a six-circle κ diffractometer. *J. Appl. Cryst* 32,943-950.
22. Thorkildsen, G., Larsen H. B., Weckert E., Mo. F. & Mathiesen R. H.(2005) . Angle calculations for a six-circle κ diffractometer. *J. Appl. Cryst* 61,460-470.

Disclaimer/Publisher's Note: The statements, opinions and data contained in all publications are solely those of the individual author(s) and contributor(s) and not of MDPI and/or the editor(s). MDPI and/or the editor(s) disclaim responsibility for any injury to people or property resulting from any ideas, methods, instructions or products referred to in the content.